Interplay Between Loop Extrusion and Compartmentalization During Mitosis

Neil Chowdhury
Phillips Exeter Academy
Exeter, NH, USA

Mentor: Sameer Abraham
Massachusetts Institute of Technology
Cambridge, MA, USA

Interplay Between Loop Extrusion and Compartmentalization During Mitosis

Author: Neil Chowdhury, **Mentor**: Sameer Abraham

Abstract

During mitosis, DNA changes its physical structure from diffuse chromatin spread throughout the cell nucleus to discrete, compacted, cylindrical chromatids. This process is essential for cells to be able to transfer replicated chromosomes to the daughter nuclei. During interphase, chromatin is compartmentalized into heterochromatin and euchromatin, resulting in a visible signal in Hi-C contact maps. However, as the cell enters mitosis, this signal is disrupted, only to reappear after the cell divides. This paper explores the interphase and mitotic states by modeling DNA using polymer simulations. It is shown that loop extrusion, the mechanism underlying mitotic chromosome formation, can simultaneously be responsible for disrupting compartmentalization.

Keywords: Hi-C, mitosis, genome architecture, molecular dynamics simulations

Table of Contents

Introduction

Chromatin is the complex of DNA and its associated proteins that exists in the cell nucleus. It is responsible for packing the cell's genetic information into an organized structure that can facilitate gene transcription and regulation.

For a cell to successfully divide, it must replicate every chromosome and then move each copy into its daughter cell with high accuracy and reproducibility. DNA replicates during the S-phase of the cell cycle, but its physical reorganization and redistribution occur during mitosis.

Mitosis can be divided into distinct phases: prophase, prometaphase, metaphase, anaphase, and telophase. During the first two stages of mitosis (prophase and prometaphase), chromatin is condensed nearly 100-fold, and individual chromosomes become visible under a microscope as rod-like structures known as chromatids (Figure 1A). This process allows for efficient separation of the duplicated DNA as each copy forms a distinct rod (Goloborodko, Marko, and Mirny 2016).

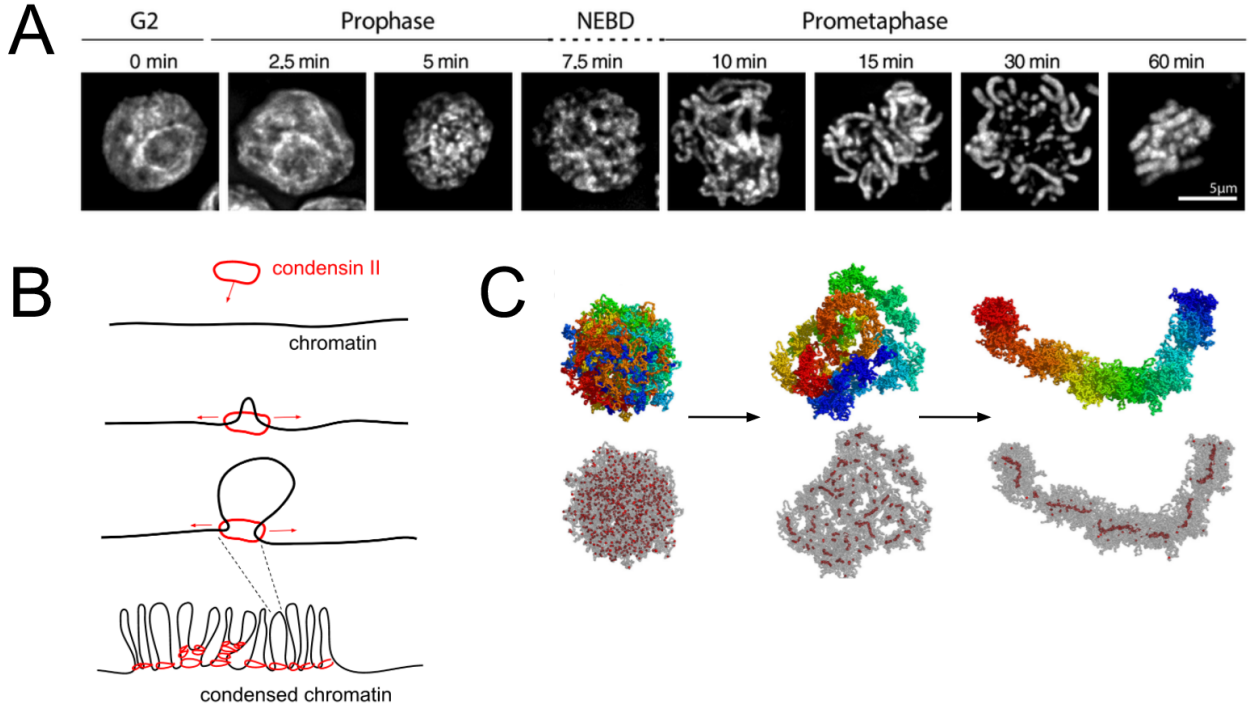

Figure 1. A: Evolution of chromatin from the interphase phenotype to the mitotic phenotype. Chromosomes separate in prophase. Taken from (Gibcus et al. 2018). B: Loops created by condensin II compact mitotic chromatin 1-dimensionally. C: Loop extrusion has been previously found to cause chromatin to compact into a mitotic chromosome phenotype in simulations. Images taken from (Goloborodko, Marko, and Mirny 2016).

The mechanism underlying the condensation of chromatin is loop extrusion (Alipour and Marko 2012), where a loop extruding factor (LEF) binds to chromatin fiber and processively creates larger loops before unbinding. When many LEFs are allowed to act on chromatin, stacked arrays of loops form and chromatin becomes organized into cylindrical mitotic chromosomes (Figure 1B). In simulations, loop extrusion has been shown to create mitotic chromosomes (Figure 1). Currently, it is understood that two protein complexes, condensin I and condensin II, play the role of LEFs during mitosis. Condensin II forms helically arranged loop arrays, while condensin I creates smaller loops that further condense the DNA (Gibcus et al. 2018).

The spatial organization of chromatin can be measured using a Hi-C experiment (Lieberman-Aiden et al. 2009). Hi-C probes genome structure by recording when two genetic loci are in proximity, known as a ***contact***. These contacts are read using sequencing and combined to create a ***contactmap***, a square matrix showing the ***contact frequency*** between all pairs of loci (Pal, Forcato, and Ferrari 2019). Rows and columns each correspond to a genetic locus; cells correspond to the contact frequency between the loci indicated by the row and column. When Hi-C contactmaps are plotted, darker cells correspond to higher contact frequencies. Figure 2 shows the Hi-C contactmap for a 20-million-base pair segment of chromosome 2 during interphase. The pixel intensities are shown on a logarithmic scale to visualize the full dynamic range of the Hi-C experiment. The predominant trend that appears in all contactmaps is that average interaction frequency decays as one moves further away from the main diagonal. This phenomenon, known as the ***scaling of contact probability***, encodes the fact that points closer to each other on a long molecule like chromatin inherently have a higher chance of being proximal to each other (Figure 2, bottom row) (Oluwadare, Highsmith, and Cheng 2019).

Hi-C contactmaps extracted from cells in interphase and mitosis contain significant differences. Interphase contactmaps display a variety of features, reflecting the presence of multiple levels of organization in the cell. At small scales, DNA is organized into loops and topologically associating domains (TADs) dependent on the action of cohesin (Schwarzer et al. 2017). At large scales, a checkerboarding signal is observed, reflecting the compartmentalization of DNA into two major compartment types: A (euchromatin) and B (heterochromatin). The genome consists of alternating A and B domains that tend to be spatially segregated. Different affinities between euchromatin (A) and heterochromatin (B) cause A-A and B-B interactions to be stronger while making A-B interactions weaker, which leads to a checkerboarding pattern. On a global scale, B domains tend to occupy the nuclear periphery, while A domains occupy the interior, although inverted architectures have also been observed. Work investigating

the underlying mechanism suggests that compartmentalization results from attraction between B domains and between B and the nuclear lamina (Falk et al. 2019).

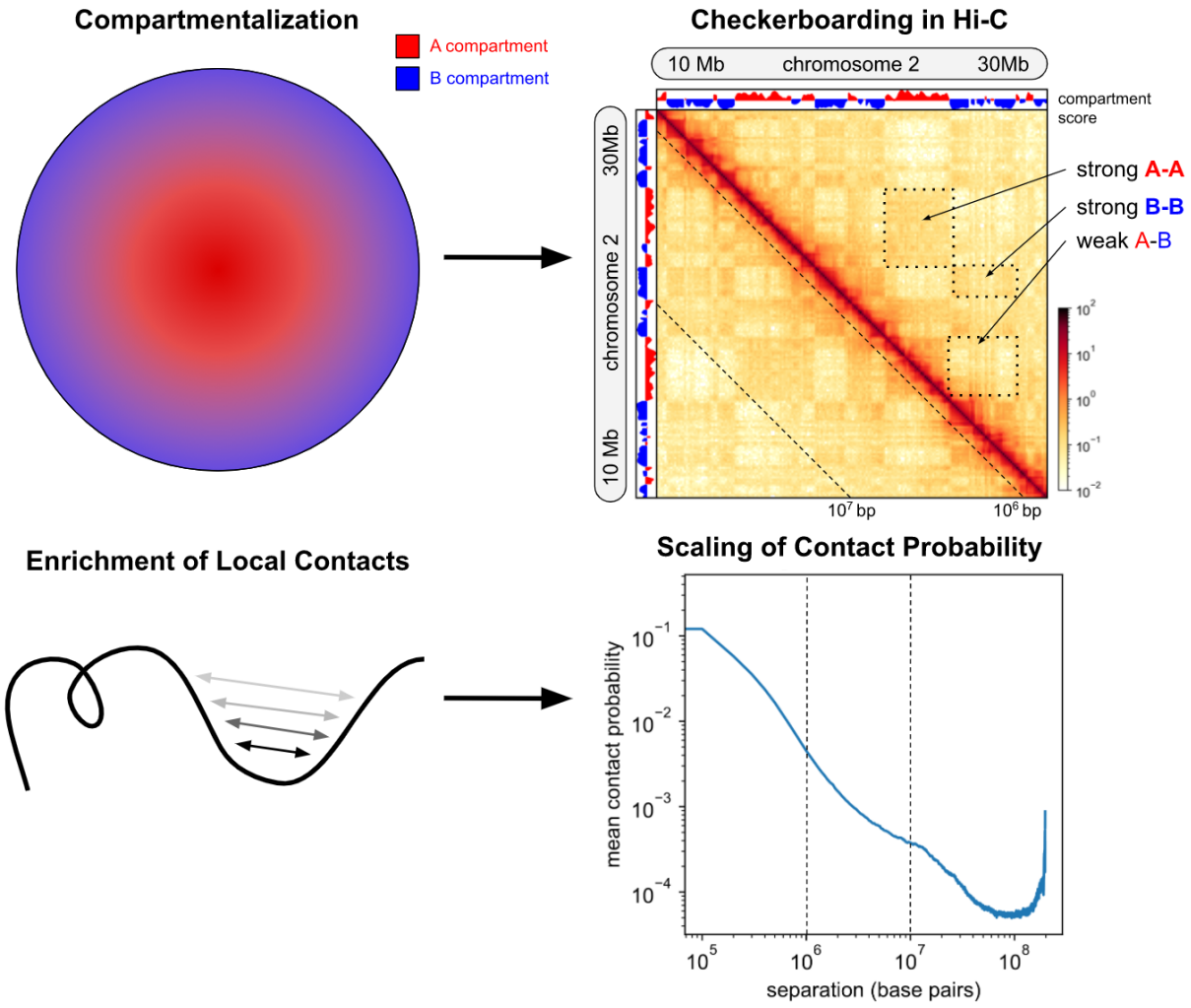

Figure 2. Compartmentalization between A and B domains (top left) leads to checkerboarding in a Hi-C contactmap (top right). A-A and B-B interactions are stronger, while A-B interactions are weaker, causing a checkerboarding pattern to appear. Contacts between nearby loci are enriched (bottom left), causing mean contact probability to decrease moving away from the main diagonal (bottom right). The Hi-C contactmap was created from data in (Gibcus et al. 2018).

By contrast, contactmaps of cells undergoing mitosis lack most of the features observed in interphase. The scaling of contact probability undergoes rapid change, representing the phenotypic changes observed in microscopy. Interestingly, compartmentalization begins to decrease in intensity at the onset of prophase and mostly disappears around

ten minutes into prophase (Gibcus et al. 2018). Furthermore, Gibcus et al. showed that this removal is reduced when condensins are not present in the nucleus.

The exact mechanism behind the disappearance of compartments in mitosis remains unknown. Although any of the biochemical changes that occur at the onset of mitosis could be responsible for the disappearance of compartments, it is clear that condensins and loop extrusion also play a role. Previous work studying interphase chromatin using polymer simulations showed that cohesin-mediated loop extrusion has a weakly antagonistic effect on compartmentalization (Nuebler et al. 2018). However, prophase is very different from interphase, as much higher levels of extrusion are present in mitosis. The effect of high levels of loop extrusion on compartmentalization in mitotic chromosomes remains unknown. In this paper, a simulation model is presented that suggests that enhanced extrusion is one factor that causes the compartmentalization pattern to disappear.

Results

Analysis of Hi-C data reveals that both condensin I and II aid the disappearance of compartments in prophase

In order to understand the effect of condensins on compartments in Hi-C, the published dataset in Gibcus et al. was reanalyzed. This dataset contained Hi-C libraries for wild-type (WT) DT-40 cells, a cell line derived from chickens. Gibcus et. al. used the auxin-inducible degron (AID) system to rapidly degrade different subunits of the condensin complex and study the corresponding change in chromosome organization (Nishimura et al. 2009). The sub-units targeted were CAP-H, CAP-H2 and SMC2; their degradation resulted in cells that lacked condensin II, condensin I, or both, respectively. For each of these mutants, the dataset contained Hi-C contact maps for interphase (G2) and synchronized timepoints 2.5, 5, 7.5, 15 and 30 minutes into mitosis.

Compartmentalization appears as increased contact frequency between A regions and between B regions, but decreased contacts between A and B regions. The A/B compartment identities themselves were identified using eigenvector decomposition (Maxim Imakaev et al. 2012). To quantify compartment disappearance, observed-over-expected (O/E) contact frequencies between AA, AB, and BB were calculated (Yardımcı and Noble 2017). In this method, the number of observed contacts between two loci was divided by the expected number of contacts based on the genomic distance between the loci, countering the scaling of contact probability. As shown in Figure 3, AA and BB have higher contact frequencies than AB during

interphase (G2), indicating that A and B compartmentalize separately. A checkerboard appears in the interphase Hi-C map.

This metric of compartmentalization was applied to the wild-type DT-40 cells from (Gibcus et al. 2018)) and the mutants lacking condensin I, condensin II and both. In wild-type DT-40 cells, AA and BB decrease in strength in the first 10 minutes of mitosis and remain constant past 10 minutes (Figure 3, row 1). In interphase, the Hi-C map contains checkerboarding, indicative of compartmentalization. However, 5 minutes into mitosis, the checkerboarding is replaced by a strong diagonal stripe, showing that the compartmentalization disappears. By comparison, in cells where only either condensin I or condensin II were present (Figure 3, rows 2-3), rates of decay of AA and BB signals were slower than the WT. For example, the cell containing only condensin I displayed a checkerboard pattern at 5 minutes. Compartments weakened in cells where both condensins were removed (Figure 3, row 4), but a non-zero signal persisted even 15 minutes into mitosis.

Therefore, both condensin I and condensin II seem to individually enhance the loss of compartment signal during mitosis. When acting together, their effect on compartments appears additive.

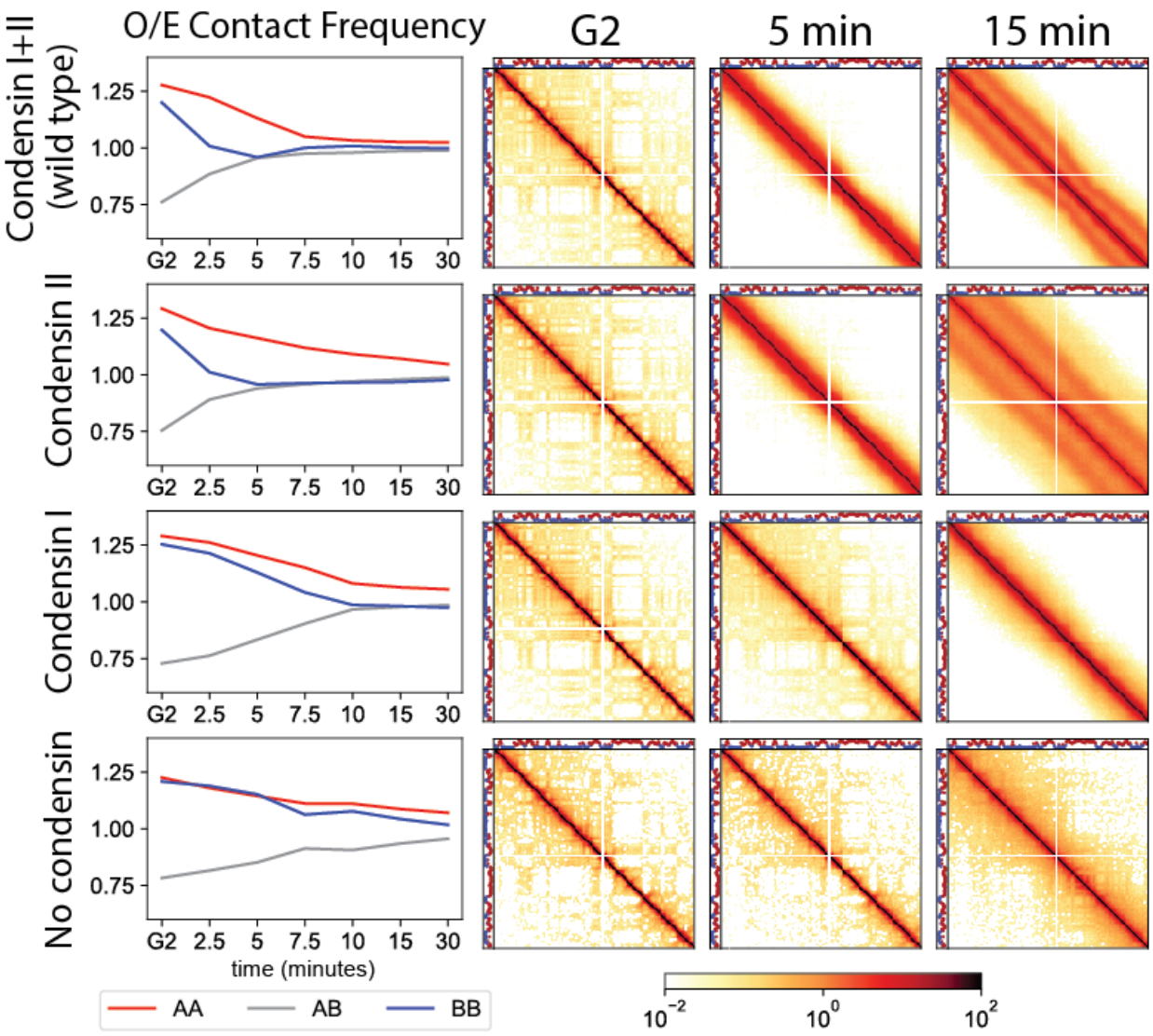

Figure 3. Compartment data for four cell lines: condensin I and II (wild type), condensin II, condensin I, and no condensin. Averaged contact frequencies of AA, AB, and BB are shown over time. AA and BB decrease, while AB increases, indicating that compartmentalization is lost. Hi-C maps of Chromosome 1, 30-60Mb are shown at G2, 5 minutes into prophase, and 15 minutes into prophase. Compartment score is indicated on the top and left side of the Hi-C maps, dividing chromatin into the A (red) and B (blue) compartments. Created from data in (Gibcus et al. 2018).

Polymer simulations show that high levels of loop extrusion weaken compartmentalization in prophase

In order to understand the mechanism underlying the condensin-dependent loss of compartments, polymer simulations were used to reproduce the effect of condensins. A

toy model of the cellular nucleus was created by confining 10 chromosomes inside a spherical nucleus. Each chromosome was represented by a polymer chain containing a random assortment of A and B domains. Attraction was added between B domains to simulate heterochromatin-heterochromatin affinity, which led to compartmentalization. Loop extruding condensins were modeled as additional non-equilibrium bonds between pairs of monomers. For the sake of simplicity, no distinction was made between condensin I and II. Simulations were run with and without loop extrusion.

Simulation results were assessed in two ways: (1) polymer conformations generated by the simulation were visually inspected to view overall trends in spatial organization, and (2) synthetic Hi-C maps were generated and compared to real data. Figure 4 shows the result of these simulations. In the absence of loop extrusion, chromosomes were highly mixed and clear spatial segregation between A and B monomers was observed. Synthetic Hi-C maps of this scenario exhibit a clear checkboarding pattern associated with compartmentalization. In contrast, chromosomes in the simulation with loop extrusion were condensed into rods (in agreement with the literature) and occupied distinct regions in the nucleus. Compartmentalization was also disrupted, as evident in contact maps and the spatial distribution of A and B monomers.

Closer inspection of polymer conformations revealed a redistribution of monomers in the nucleus in the presence of extrusion. This effect was quantified by plotting monomer densities for A and B type monomers as a function of radial position in the nucleus. In addition to the condensation of chromosomes, extrusion induces an outward radial shift of monomers. This initial result provides qualitative evidence that the loop extrusion in mitotic chromosomes can both disrupt compartmentalization and cause unexpected effects on the global organization of chromosomes in the nucleus.

The system of compartments and loop extrusion was more thoroughly examined by sweeping the extrusion parameters and analyzing the results. Goloborodko, Marko and Mirny (2016) showed that loop extrusion is characterized by two main parameters: ***lifetime*** and ***separation*****.** Lifetime is the average number of extrusion simulation steps a condensin takes before unbinding from the polymer, and separation is the inverse of the average density of condensins bound to the polymer chain at any time. Generally, decreasing separation and increasing lifetime will strengthen the effects of extrusion on the overall organization of the polymer it acts upon (Nuebler et al. 2018).

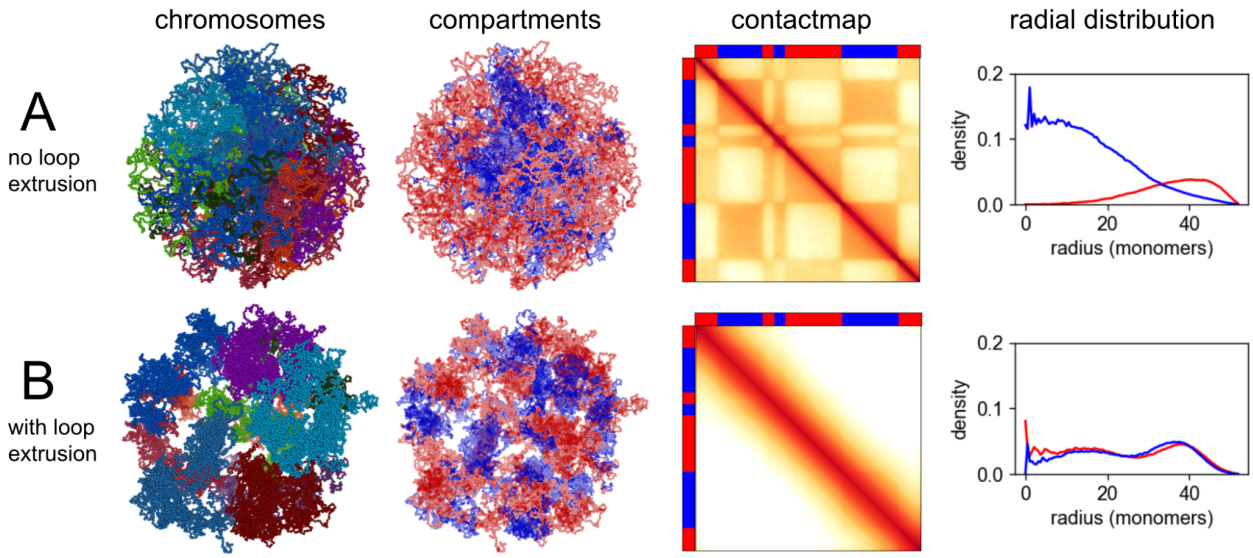

Figure 4. Row A shows the model without loop extrusion, while Row B shows the effect of loop extrusion. Chromosomes (rainbow) condense and separate when loop extrusion is added. Compartments (red: A, blue: B) are disrupted by loop extrusion. The contactmaps, plotted with compartment labels on the top and left (red: A, blue: B) show that checkerboarding disappears when loop extrusion is added. The final column shows the radial density distribution of A (red) and B (blue), in units of monomers per cubic nanometer. The distributions become nearly equal when loop extrusion is added, and monomers appear to move outward. The condensin lifetime was 50 and separation was 25.

Simulations for various condensin lifetimes and separations were run, and contactmaps were extracted to assess the results (Figure 5). The range of parameters was chosen such that lifetime is greater than separation since literature has shown that the mitotic phenotype emerges in this region of the parameter space (Goloborodko, Marko, and Mirny 2016). The results demonstrate that the degree of compartment washout depends on both the lifetime of condensin and the separation between condensins. Several parameter-dependent trends were also observed.

Lower separation (i.e., more condensins in the system) leads to a weaker compartments, showing that an increased amount of extrusion leads to increased disruption of compartmentalization. When loop extrusion is added, the checkerboarding pattern reflective of compartmentalization disappears (Figure 5). In addition, longer lifetimes lead to stronger compartmental signals near the main diagonal (short distances). This can be explained by the fact that longer lifetimes result in longer loops, and once a loop is formed, the monomers within the loop can recompartmentalize.

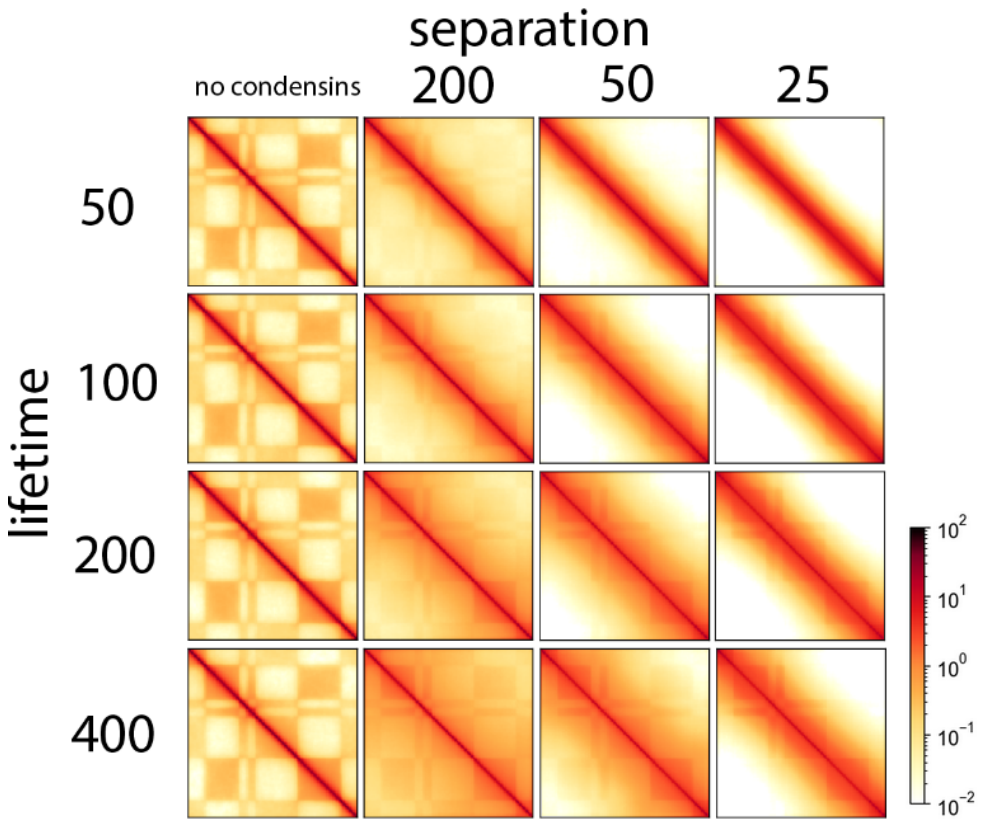

Figure 5. Contactmaps of simulations with B-B attraction (0.3 kT), varying lifetime and separation. The first column shows simulations with no loop extrusion. When loop extrusion is added and separation decreases, the checkerboarding pattern vanishes beyond a narrow diagonal. Increased condensin lifetime causes the diagonal to widen and retain compartmentalization features.

The effect of loop extrusion on the large-scale organization of chromatin was explored. Figure 6 shows that without extrusion, B monomers naturally condense in the center of the nucleus (r = 0), while A monomers are distributed at the periphery (r ≈ 40). This separation is an inverse of the traditional compartmentalization of B on the periphery and A in the center because B-lamina attraction is not present. When loop extrusion is added, both A and B monomers migrate toward the periphery, and this effect is primarily modulated by condensin separation. Additionally, as condensin separation decreases, the radial distributions of A and B monomers become equal.

Together, these analyses show that loop extrusion in the mitotic regime is effective at removing the spatial organization caused by compartmentalization, and the separation between condensins predominantly controls that compartment removal. Closely packed loops may cause polymers to form bottlebrush-like conformations, which contain a main chain with several smaller side chains. Bottlebrushes have been shown to avoid

entangling with other bottlebrush polymers, which could inhibit B-B interactions and remove the compartmental signal (Daniel et al. 2016).

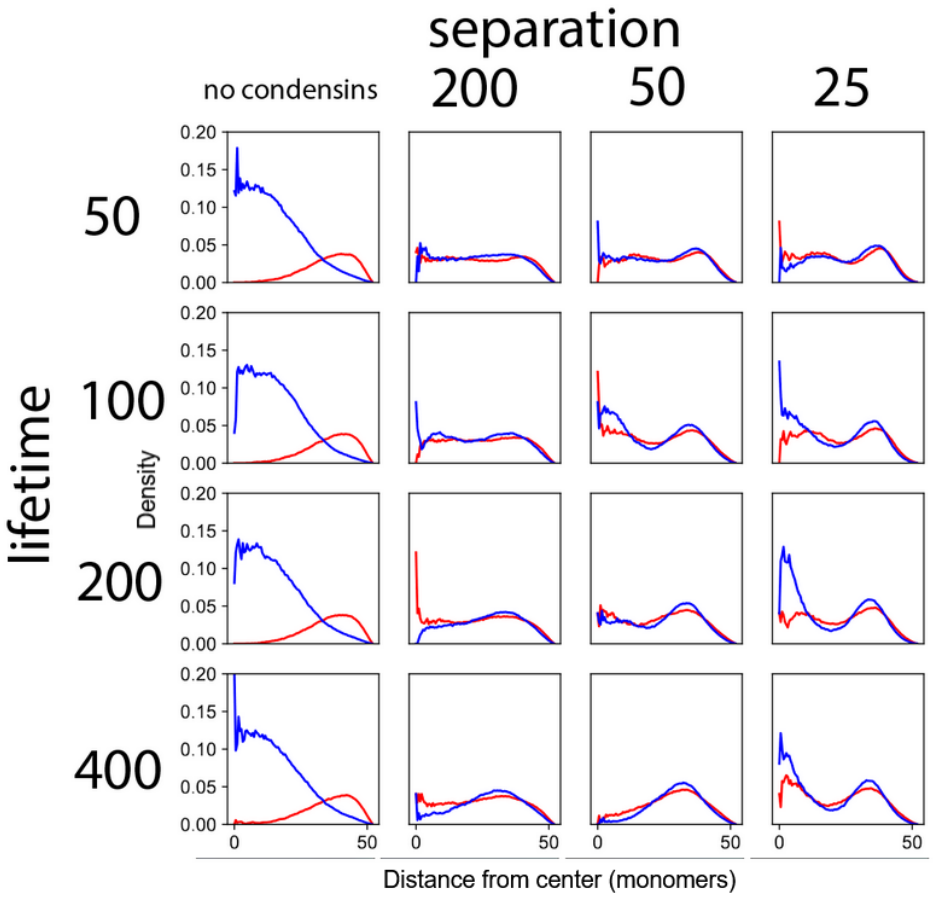

Figure 6. The density of A (red) and B (blue) monomers, measured by the radius from the center (0, 0, 0) of the conformation. Without loop extrusion, B monomers are clustered near the center, and A monomers are clustered near the periphery. When loop extrusion is added, the radial distributions become nearly equivalent.

An additional parameter was significant when considering the interplay between loop extrusion and compartmentalization: the speed of extrusion. The speed of extrusion can be measured relative to the natural speed of polymer dynamics. In cells, chromatin itself moves within the nucleus over a specific timescale, which determines the rate at which compartmentalization occurs. If the extrusion is fast compared to this timescale, it will change the conformation of chromatin faster than the chromatin can react. Thus, constant, fast extrusion can prevent the reemergence of compartments and contribute to its disappearance.

The effect of condensin speed was explored. In simulations, the polymer is allowed to relax for a period between extrusion steps. The simulation proceeds for a certain fixed

number of steps while the extrusion bonds are fixed in place. The smaller the number of these steps, the faster extrusion is relative to the polymer motion. Figure 7 shows that as the number of steps increases (condensin speed decreases), long-range compartmental interactions become stronger. Since loop extrusion causes heterochromatin and euchromatin to mix, faster loop extrusion speed aids in removing compartmentalization during mitosis.

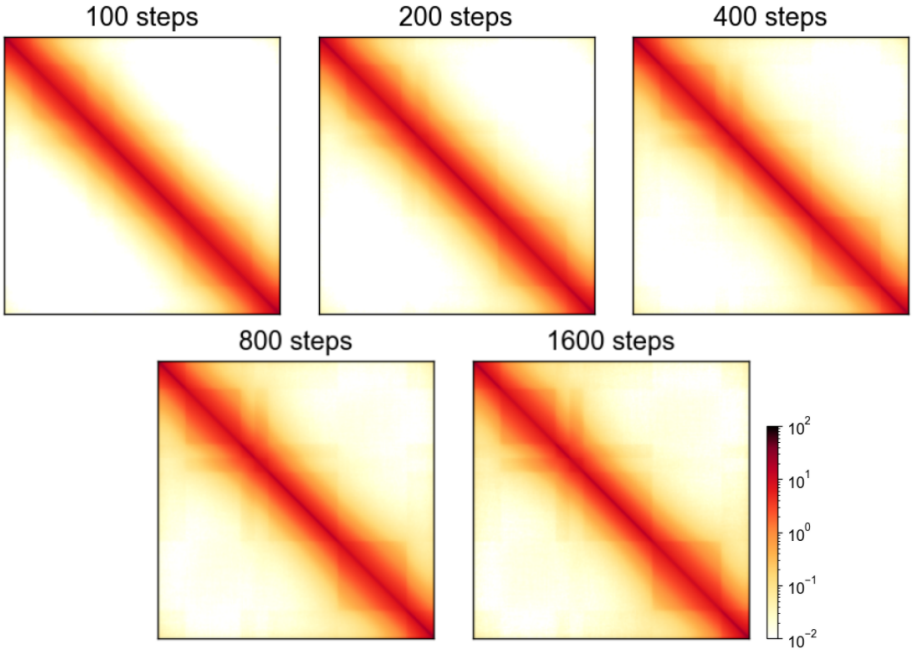

Figure 7. Contactmaps from simulations with varying loop extrusion speed, run with a condensin lifetime of 50 and separation of 25. Speed is inversely proportional to the number of molecular dynamics (MD) steps per loop extrusion step. As the number of MD steps increases, loop extrusion speed decreases and the compartmental signal becomes stronger.

Adding loop extrusion disrupts lamina-induced compartmentalization

Past studies have concluded that compartmentalization is caused by two forces: heterochromatin-heterochromatin attraction, and heterochromatin-nuclear lamina attraction. The nuclear lamina occupies the periphery of the cell nucleus, so attraction between lamina and heterochromatin causes heterochromatin to surround a center of euchromatin, as seen in Figure 2. A simulation was created with no loop extrusion to model interphase chromatin (Figure 8A). The A and B compartments are segregated, with B occupying the nuclear periphery and A in the center. In this state, the chromosomes themselves are spread over large parts of the cell nucleus.

However, when loop extrusion is added (Figure 8B), the chromatin again compacts into discrete rods. This reflects the mitotic phenotype, as the chromosomes occupy distinct positions around the outside of the cell. The A/B segregation is also disrupted, as B domains no longer surround A.

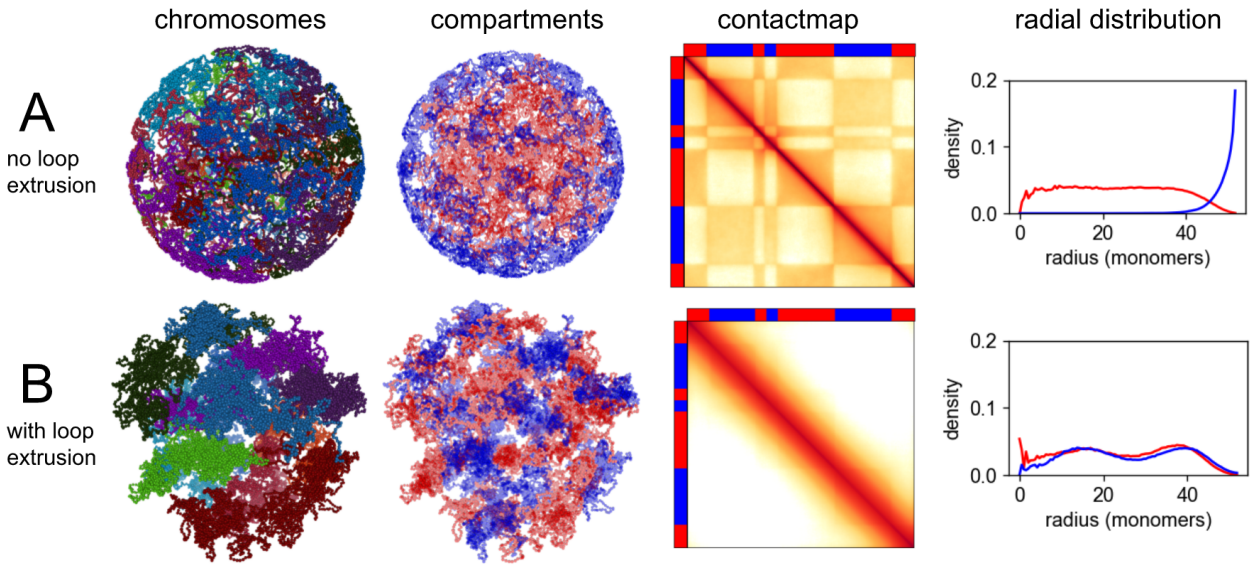

Figure 8. Row A shows the model without loop extrusion, while Row B shows the effect of loop extrusion. Chromosomes (rainbow) condense and separate when loop extrusion is added. Compartments (red: A, blue: B) are disrupted by loop extrusion, and the spherical shell of B monomers surrounding A is removed. The contactmaps and radial density distribution are plotted with compartment labels (red: A, blue: B), and they both illustrate that compartmentalization disappears when loop extrusion is added. The condensin lifetime was 50 and separation was 25.

Figure 9 quantitatively shows that the lamina attraction is disrupted. Without extrusion, B monomers have their density concentrated at the farthest distance from the center of the nucleus. However, when cohesins are added (separation decreases), the B monomers attain a density distribution similar to A monomers. Lowering condensin lifetime also helps make the A and B density distributions equivalent. Therefore, rapid loading/unloading of condensins onto chromosomes might increase its ability to avoid compartmentalizing.

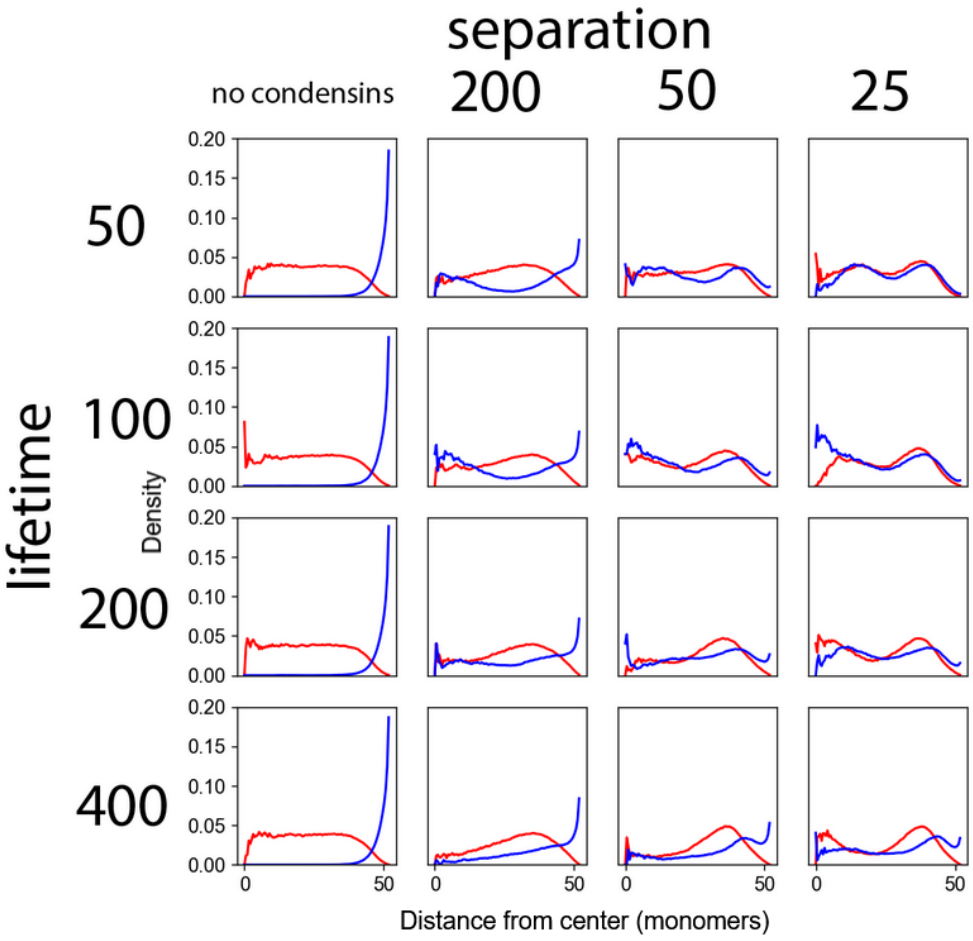

Figure 9. Radial density plots (A: red, B: blue) for several simulations with B-lamina attraction (1.2 kT) and B-B attraction (0.3 kT), varying condensin lifetime and separation.

Conclusion

Increasing the strength of loop extrusion in simulations causes chromosomes to compact and separate, similarly to the mitotic phenotype. Loop extrusion can disrupt the effects of compartmentalization caused by B-B and B-lamina attraction, which could explain why wild-type cells exhibit a stronger loss in compartments than cells in which condensins were degraded. This provides further evidence that condensins facilitate loop extrusion in order to compact chromatin in preparation for mitosis.

This paper also advances the study of the interplay between compartmentalization and loop extrusion through polymer simulations. The forces presented can model heterochromatic interactions, the effects of loop extrusion, and the physics of mitotic chromosomes, all at high resolution. To the author's knowledge, this is the first

simulation of compartments in mitotic chromosomes. Analyzing the results of these simulations will enhance our understanding of how cells regulate genome structure, an essential area of cell biology.

Methods

Polymer model setup

Each chromosome is modeled as a chain of 3,000 monomers. Ten chromosomes are confined inside a sphere, which represents the cell nucleus. The simulation model is based on the open-source OpenMM library, which integrates user-defined forces to determine the position of each monomer after fixed timesteps (Eastman et al. 2017). The Polychrom library was used to construct the OpenMM forces and polymer chain parameters (Maksim Imakaev, Goloborodko, and hbbrandao 2019).

Energies are in units of kT; distances are measured in terms of the diameter of monomers (20 nm).

Simulating compartmentalization

In cells, A-B compartmentalization is driven by attraction within heterochromatin (Falk et al. 2019). Each of the monomers is labeled as either “A” or “B” depending on whether it represents euchromatin or heterochromatin, respectively. The smooth square well force adds a repulsive potential well when two monomers are less than 1 diameter apart and an attractive well (with depth equal to the B-B attraction energy) when the monomers are separated by 1 to 1.5 diameters (Figure 10A). Increasing the attraction energy increases the strength of compartmentalization.

Simulating the nuclear lamina

The nuclear lamina is positioned on the sphere of confinement in the simulation. B monomers experience attraction to a spherical wall at a fixed radius $r = r_0$. The energy of attraction, $U(r)$, can be defined in terms of the radial distance of the monomer, r, as shown in Figure 10B. The potential itself is sinusoidal, and its minimum value (at r_0) is the B-lamina attraction energy.

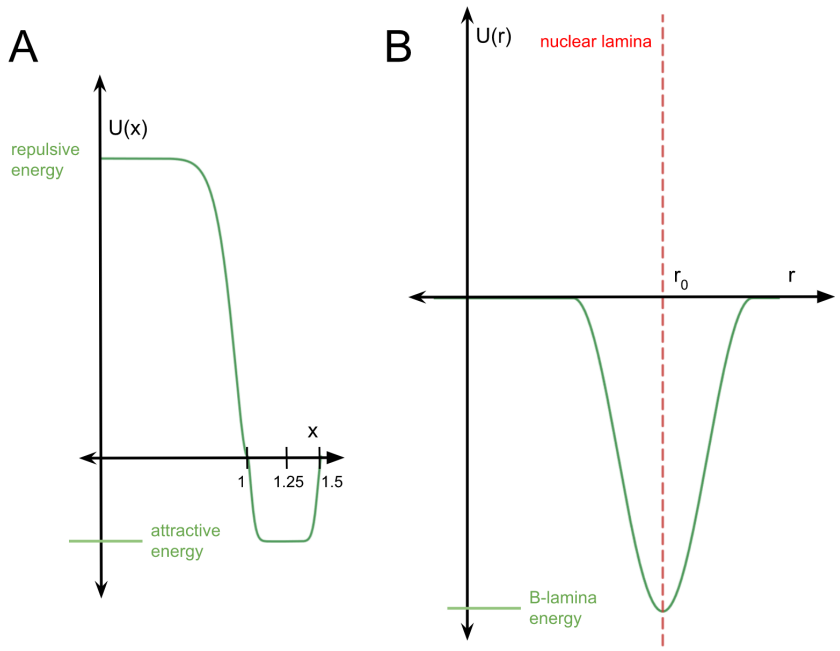

Figure 10**.** The energy functions for compartmentalization and lamina attraction. A: The smooth square well potential for modeling compartment attraction between two monomers separated by a distance *x*. B: The spherical well potential for a monomer at radius *r*.

Simulating loop extrusion

Condensins are modeled as harmonic bonds that connect two monomers on a chromosome, known as the two legs. One leg moves upstream while the other leg moves downstream. For example, a condensin connecting monomers (i, j) in one timestep will connect (i-1, j+1) in the next loop extrusion step, as illustrated in Figure 11. A condensin leg stops extruding when it is obstructed by the leg of another condensin, making it stalled, but the other leg may continue to extrude.

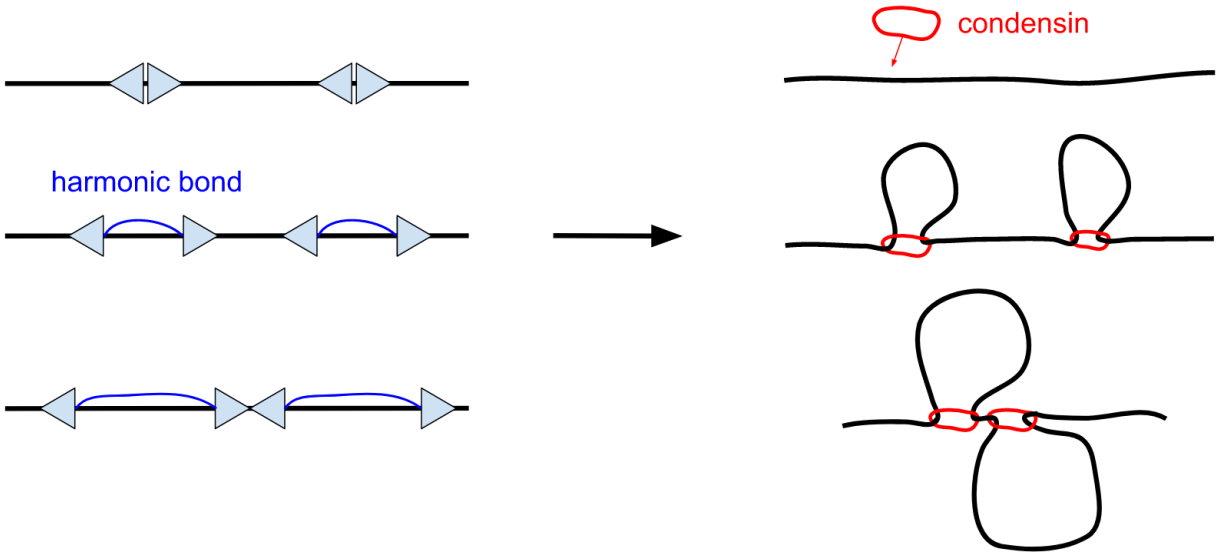

Figure 11. In the simulation, condensins are modeled as harmonic bonds connecting pairs of monomers, stretching longer distances as time progresses. The bonds create loops in the polymer chain.

Condensins were randomly loaded onto the genome and unloaded each timestep with probability 1/λ, to have an overall lifetime of λ. The number of condensins (N/d) remained constant over the entire simulation. To maintain this number, a condensin was loaded onto the polymer at a random, vacant position (i, i+1) every time a condensin was unloaded.

Acknowledgments

I would like to thank my mentor, Sameer Abraham, for providing valuable suggestions throughout my project and giving feedback on my data analysis and simulations. I would also like to thank Maxim Imakaev, who mentored me last year and taught me how to create polymer simulations with loop extrusion and compartmentalization. I thank Professor Leonid Mirny for valuable discussions about my project and further guidance. Finally, I am very grateful that MIT PRIMES has given me the opportunity to research computational biology in the Mirny Lab at MIT.

Bibliography

Alipour, Elnaz, and John F. Marko. 2012. “Self-Organization of Domain Structures by DNA-Loop-Extruding Enzymes.” *Nucleic Acids Research* 40 (22): 11202–12.

Daniel, William F. M., Joanna Burdyńska, Mohammad Vatankhah-Varnoosfaderani, Krzysztof Matyjaszewski, Jarosław Paturej, Michael Rubinstein, Andrey V. Dobrynin, and Sergei S. Sheiko. 2016. “Solvent-Free, Supersoft and Superelastic Bottlebrush Melts and Networks.” *Nature Materials* 15 (2): 183–89.

Eastman, Peter, Jason Swails, John D. Chodera, Robert T. McGibbon, Yutong Zhao, Kyle A. Beauchamp, Lee-Ping Wang, et al. 2017. “OpenMM 7: Rapid Development of High Performance Algorithms for Molecular Dynamics.” *PLoS Computational Biology* 13 (7): e1005659.

Falk, Martin, Yana Feodorova, Natalia Naumova, Maxim Imakaev, Bryan R. Lajoie, Heinrich Leonhardt, Boris Joffe, et al. 2019. “Heterochromatin Drives Compartmentalization of Inverted and Conventional Nuclei.” *Nature* 570 (7761): 395–99.

Gibcus, Johan H., Kumiko Samejima, Anton Goloborodko, Itaru Samejima, Natalia Naumova, Johannes Nuebler, Masato T. Kanemaki, et al. 2018. “A Pathway for Mitotic Chromosome Formation.” *Science* 359 (6376). https://doi.org/10.1126/science.aao6135.

Goloborodko, Anton, John F. Marko, and Leonid A. Mirny. 2016. “Chromosome Compaction by Active Loop Extrusion.” *Biophysical Journal* 110 (10): 2162–68.

Imakaev, Maksim, Anton Goloborodko, and hbbrandao. 2019. *Mirnylab/polychrom: v0.1.0*. https://doi.org/10.5281/zenodo.3579473.

Imakaev, Maxim, Geoffrey Fudenberg, Rachel Patton McCord, Natalia Naumova, Anton Goloborodko, Bryan R. Lajoie, Job Dekker, and Leonid A. Mirny. 2012. “Iterative Correction of Hi-C Data Reveals Hallmarks of Chromosome Organization.” *Nature Methods* 9 (10): 999–1003.

Lieberman-Aiden, Erez, Nynke L. van Berkum, Louise Williams, Maxim Imakaev, Tobias Ragoczy, Agnes Telling, Ido Amit, et al. 2009. “Comprehensive Mapping of Long-Range Interactions Reveals Folding Principles of the Human Genome.” *Science* 326 (5950): 289–93.

Nishimura, Kohei, Tatsuo Fukagawa, Haruhiko Takisawa, Tatsuo Kakimoto, and Masato Kanemaki. 2009. “An Auxin-Based Degron System for the Rapid Depletion of Proteins in Nonplant Cells.” *Nature Methods* 6 (12): 917–22.

Nuebler, Johannes, Geoffrey Fudenberg, Maxim Imakaev, Nezar Abdennur, and Leonid A. Mirny. 2018. “Chromatin Organization by an Interplay of Loop Extrusion and Compartmental Segregation.” *Proceedings of the National Academy of Sciences of the United States of America* 115 (29): E6697–6706.

Oluwadare, Oluwatosin, Max Highsmith, and Jianlin Cheng. 2019. “An Overview of Methods for Reconstructing 3-D Chromosome and Genome Structures from Hi-C Data.” *Biological Procedures Online* 21 (April): 7.

Pal, Koustav, Mattia Forcato, and Francesco Ferrari. 2019. “Hi-C Analysis: From Data Generation to Integration.” *Biophysical Reviews* 11 (1): 67–78.

Schwarzer, Wibke, Nezar Abdennur, Anton Goloborodko, Aleksandra Pekowska, Geoffrey Fudenberg, Yann Loe-Mie, Nuno A. Fonseca, et al. 2017. “Two

Independent Modes of Chromatin Organization Revealed by Cohesin Removal." *Nature* 551 (7678): 51–56.
Yardımcı, Galip Gürkan, and William Stafford Noble. 2017. "Software Tools for Visualizing Hi-C Data." *Genome Biology* 18 (1): 26.

Declaration of Academic Integrity

The participating team declares that the paper submitted is comprised of original research and results obtained under the guidance of the instructor. To the team's best knowledge, the paper does not contain research results, published or not, from a person who is not a team member, except for the content listed in the references and the acknowledgment. If there is any misinformation, we are willing to take all the related responsibilities.

Names of team members: Neil Chowdhury

Signatures of team members 

Name of the instructor: Sameer Abraham

Signature of the instructor

Date 9/15/2021